Biochemistry and Biophysics Reports 12 (2017) 172–184

Contents lists available at ScienceDirect

Biochemistry and Biophysics Reports

journal homepage: www.elsevier.com/locate/bbrep

Selenium nanoparticles induce suppressed function of tumor associated macrophages and inhibit Dalton's lymphoma proliferation

Pramod Kumar Gautam[a,b,*], Sanjay Kumar[a], M.S. Tomar[a], Rishi Kant Singh[a], A. Acharya[a], Sanjay Kumar[b], B. Ram[b]

[a] Institute of Science, Department of Zoology, Faculty of Science, Banaras Hindu University, Varanasi, India
[b] Department of Drayaguna, Faculty of Ayurveda, Institute of Medical Science, Banaras Hindu University, Varanasi, India

ARTICLE INFO

Keywords:
Selenium nanoparticle
TAMs
Lymphoma
ROS
Anti-tumor function

ABSTRACT

Selenium Nanoparticle (SeNPs) is reported that it enhances and maintains optimal immune during infection and malignancies. To this end, we examined the role of selenium on TAMS whose anti-tumor function suppressed which favor tumor progression. BALB/c (H2d) strain of mice non-Hodgkin type of Dalton's cell line was used to check the role of carboxlic group induced, synthesized SeNPs on TAMs. Screening of IC50 value was done primarily trypen blue exclusion assay and 50% proliferation of DL cells inhibited 40 ng/ml to 50 ng/. Treatment also decreases ΔΨm, fragmentation of DNA of DL cells and arrest cells cycle in G1/G0 phage. Untreated TAMs cells showing suppressed expression of ROS, adhesion, phagocytosis, fusion and receptor profiling such as ICAM-1, CD47, CD172α. Which was induced more as compare to untreated group. SeNPs have potential to induce the anti-tumor function of TAMs whose anti-tumor function down-regulated pliable shifted towards tumor progression. It decreased the proliferation of DL cell by inducing apoptosis. Therefore, the synthesized SeNPs could be used for imaging diagnosis and cancer therapy which must be cost effective with negligible side effects shifted towards tumor progression. It decreased the proliferation of DL cell by inducing apoptosis.

1. Introduction

Selenium (Se) is an important micronutrient with several important aspects of human health such as cardiovascular health, prevention of neurodegeneration, proper thyroid hormone metabolism, preventing cancer progression and optimal immune responses [1]. It is a structural component of the active center of many antioxidant enzymes and functional proteins. Selenium mainly consists of two inorganic forms, selenite, and selenate [2]. Selenium containing protein (selenoproteins) plays an important role in chronic inflammation and initiation of immune response and thus regarded as good anti-cancer agent. The anti-cancer potential of the Selenium has been identify on different cancer cell line. Sufficient levels of selenium are important in regulating excessive immune responses and chronic inflammation [3–5]. Moreover, antioxidative effects of Se have been shown to protect phagocytic cells and surrounding tissues from oxidative radicals produced by the respiratory chain of neutrophils and macrophages during phagocytosis [6]. The deficiency of Selenium negatively affect immune cells activation during oxidative stress, protein folding and calcium flux [7,8].

It has been observed that $CD34^+$ originated lymphoid progenitor macrophages play an important role during encounter with the cancer cells [9–11]. During tumor progression, macrophages migrated to the tumor site in the influence of vascular endothelial growth factor (VEGF),colony-stimulating factor (CSF)-1 and MIP-1α present in to the cellular microenvironment [12]. Tumors are generally characterized by nutrient deprivation, hypoxia, acidosis and aberrant stroma, and consists both malignant and non-malignant cell types that include endothelial cells, fibroblasts, and various cells derived from the bone marrow. Tumor cells release several immunosuppressive factors and pro angiogenic cytokines [13,14] and growth factors, such as VEGF, TNF-α, TNF-β, IL-1, IL-8 and bFGF (Basic fibroblast growth factor) that stimulate endothelial cell proliferation and promote the formation of [15–20] differentiated capillary tube. They also express a broad range of angiogenesis-modulating factors such as Matrix metalloproteinases (MMPs) and cyclooxygenase-2 that play a significant role in capillary formation and vascularization in the tumor masses. These tumor promoting factors further down-regulate macrophages function and change their functional phenotype M1 to altered M2 phenotype [15–24]. The M2 or tumor associated macrophages (TAMs) constitute about 10–50% of total tumor mass and serve as slaves for the tumor.

Previously, we have shown that TAMs are phenotypically and functionally altered populations of macrophages, characterized by

* Correspondence to: Department of Biochemistry, All India Institute of Medical Science, 3rd floor, PC block, New Delhi 110029, India.
E-mail addresses: gautam@aiims.edu, pramodgautam_13@yahoo.com (P.K. Gautam).

http://dx.doi.org/10.1016/j.bbrep.2017.09.005
Received 19 May 2017; Received in revised form 16 September 2017; Accepted 18 September 2017
Available online 21 September 2017

decreased cytotoxic function, reduced surface receptor expression, and enhanced production of anti-inflammatory cytokines that polarizes the immune response to favors the growth of tumor cells [20–25]. Keeping the immunomodulatory function of selenium in mind, first we characterize and optimize the dose of chemically synthesized selenium nanoparticles (SeNPs) and use to induce TAMs isolated from DL-bearing mice. Results shows that selenium effectively induces the ROS generation, formation of macrophage polykaryon, expression of adhesion molecules (CD54 or ICAM-1), and fusion receptors (CD47 & CD172α) on TAMs. Further, we also found that SeNPs decrease the tumor cell proliferation.

2. Material and method

2.1. Reagents

Selenium powder, sodium sulphite, polyvinyl alcohol (PVA),MTT and Concanavalin-A were purchased from SigmaAldrich, Bangalore, India. RPMI 1640 culture medium was obtained from HiMedia, Mumbai, India. Foetal bovine serum (FBS) was obtained from Invitrogen, CA, USA, CD47, CD172a conjugated with FITC and CD14 conjugated with PE from eBiosciences, San Diego, CA, USA. LPS, DCFH-DA, PMA, RH-123, DAPI, Hoechst 33258 and Phalloidin were obtained from Sigma Chemical Co. (St. Louis, MO, USA). Na2HPO4, KH2PO4, formaldehyde,trypsinand acetone were purchased from Qualigens, Mumbai, India. Glutaraldehydewas obtained from Serva Electrophoresis, Heidelberg, Germany. All other chemicals otherwise stated were obtained from Qualigens.

2.2. Animals and tumor model

Inbred populations of BALB/c (H2d) strain of mice of either sex and at 8–12 weeks of age were used. Mice obtained from the Departmental Animal House, Banaras Hindu University, Varanasi, India, and housed in a pathogen-free specialized small animal facility with 12 h dark-light cycle. All the animals treated with utmost human care and had free access to food and water. For tumor system, healthy mice of either sex were injected intraperitoneally (i.p.) with 1.0×10^6 non-Hodgkin type of Dalton's lymphoma (DL cells) in 0.5 ml sterile PBS and allow to grow for 18 days.

The experimental endpoint was 18th day of the tumor growth where more than 90% physical activity of the animals and ability to access food and water is lost. Mice were euthanized by cervical dislocation, a method authorized by Animal Ethical Committee, Banaras Hindu University Varanasi, India, and Animals Ethical Committee, Indian Council of Medical Research (ICMR), New Delhi for killing of experimental animals, and observed until all muscle activity and breathing has ceased for at least 120 s. No mice died before meeting the endpoints described.

2.3. Synthesis and characterization of SeNPs

2.3.1. Synthesis of SeNPs by chemical method

SeNPs were synthesized as per previously reported method from our lab (8). In brief, Selenium powder (0.25 M) was added to the solution of sodium sulphate (0.50 M) in 100 ml of double distilled water and mixture was stirred at 70 °C for 9 h. A transparent sodium selenosulphate (Na2SeSO3) solution was obtained which was used as a precursor for the synthesis of the SeNPs. Sodium selenosulphate solution (0.002 M) was used in a separate Erlenmeyer flask and 0.005 M of acetic acid was added dropwise into sodium selenosulphate solution for the carboxylic group-induced synthesis of the SeNPs. Appearance of pink color preliminary confirmed the formation of the SeNPs. The synthesized SeNPswas stabilized by 0.05 ml of 1% aqueous polyvinyl alcohol. This color indicated the synthesis of Se NPs in to the solution. Further UV spectra were taken at different time interval. After synthesis of selenium nanoparticle the whole supernatant was collected and centrifuged at 11,500 rpm for 15 min at 4 °C, supernatant was discard and pellet was washed with distilled water thrice and final pellet suspended distilled water and sonicated, and lyophilized. After that powder was collect for performing analytical techniques.

2.3.2. Ultraviolet-visible spectroscopic analysis

Synthesis of SeNPs by reducing the respective metal ions solution with Sodium citrate tribasic dehydrate ($C_6H_5Na_3O_7{\cdot}2H_2O$) easily observed by UV–vis spectroscopy. The absorption spectrums recorded and quantify metal ion concentration using Hitachi U-2910 spectrophotometer in range from 300 to 1200 nm range. Synthesized SeNPs (200–350 nm) of diameter gave sharp peak in the visible region of the electromagnetic spectrum. Spectroscopy was performed at central facility of Department of Botany, BHU, Varanasi, India.

2.3.3. Sonicatioin and Iyophilization

Samples were observing under UV–vis spectroscopy, synthesized sample further perform sonications which facilitate equal size fragmentation. In brief, sample were kept in the ice in 20 ml of centrifuge tube and provide ultrasonic vibration for the 2 min with the time gap of 30 s/cycle using SONIC, Vibra Cell sonicater at central facility of Department of Botany, BHU, Varanasi, India. Further sample was lyophilize using Christ Alpha 1–2 lyophilizer for preparation of powdered SeNPs for further standardization and characterization.

2.3.4. Fourier transform infrared (FTIR) analysis

FTIR measurements of the powdered purified SeNPs were assessed using Perkin Elmer, Spectrum Two FTIR (Waltham, MA, USA) system in the diffused reflectance mode. In order to identify the possible reducing and stabilizing molecules in Sodium citrate solution, FTIR analysis was carried out. The spectral range from 400 to 4000 cm^{-1} with resolution of 4 cm^{-1} powder samples for the FTIR was similarly as for powder diffraction measurements. The FTIR spectra of base material (Sodium citrate solution) taken before and after synthesis of SeNPs were analyzed to study the possible functional for the formation of SeNPs.

2.3.5. X-ray diffraction (XRD) analysis

To determine the structural characterization of SeNPs by using X-ray diffraction (X'Pert Pro PANalytical, ALMELO, Netherlands) at central facility of Department of Physics, BHU, Varanasi, India. To obtain XRD patterns of the SeNPs, NPswere subjected to XRD analysis at 45 kV and 40 mA with 2θ in therange from 0° to 80° angle. This diffraction pattern is used to identify the specimen's crystalline phases and to measure its structural properties, size and orientation of crystalline profile.

2.3.6. Thermogravimetric (TGA) analysis

The thermal stability of the SeNPs was measured by TGA. All samples were heated up to 950 °C with heating rate 30 °C/min. The initial weight loss up to 200 °C is attributed to the loss of physisorbed moisture. Thermal stability observation and characterization of samples were done at central facility of Department of Chemistry, BHU, Varanasi, India.

2.3.7. Transmission electron microscopy (TEM) analysis

TEM analysis was performed to determine the morphology, size and shape of the selenium nanoparticles. TEM measurements were done by transmission electron microscope, Tecnai 20G2 FEI, Oregon, USA. The TEM grid was prepared by placing a drop of the bio-reduced diluted solution on a carbon-coated copper grid and later drying it under a lamp. TEM facility was using at central facility of Department of Physics, BHU,Varanasi.

2.3.8. Scanning electron microscopy (SEM)

The surface observation of SeNPs samples were done by using

scanning electron microscope (Zieas-EVO LS-10) at 25 kV at LV mode at central facility of Department of Zoology, BHU, Varanasi, India. In the SEM an electron beam is focused into affine probe and subsequently raster over a small rectangular zone. As the electron beam interact with the NPs sample it creates various signals (secondary electron, internal currents, photon emission, etc.) can be detected.

2.3.9. Assay for cytotoxicity activity and dose optimization

2.3.9.1. Screening and trypen blue exclusion assay. DL cell were harvested from tumor bearing mice as described above and at a cell density of 1×10^6 in the culture medium with or without PMA and SeNPs of different concentration and incubated for time periods of 24 h in CO_2 incubator (Shella, Oregon, CA, USA). After incubation, control group viability of peritoneal macrophages was determined using exclusion by the trypan blue method. Trypan blue (final concentration of 0.01% wt/vol; Sigma Chemical Co.) was added to each experimental group of cells. Thereafter, aliquots of 10 µL were taken and cells were counted in a hemocytometer chamber. Morphologic evaluation of viable cells was performed by light microscopy (Olympus CKX 41, Center Valley, PA, USA) at 630× original magnification.

$$\%\text{cell Viability} = \frac{\text{Total number of viable cells}}{\text{Total number of cells}} X100$$

2.3.9.2. MTT assay. The cytotoxicity of samples of the DL cell (Leukemia) was determined by the MTT assay. In brief, 1×10^5/well DL cells were plated in 1 ml of medium/well in 24-well plates. After 48 h incubation the cell reaches the confluence. Then, cells were incubated in the presence of different (increasing order) concentrations of the samples in 0.1% DMSO for 48 h at 37 °C. After removal of the sample solution and washing with phosphate buffered saline (pH 7.4), 200 µL/well (5 mg/ml) of MTT solution was added for 4 h of incubation. After 4 h of incubation, 0.04 M HCl/isopropanol were added. Viable cells were determined by the absorbance at 570 nm. Measurements were performed and the concentration required for a 50% inhibition of viability (IC50) was calculated. The absorbance at 570 nm was measured with a UV- Spectrophotometer using wells without sample containing cells as blanks.

2.4. Anti-cancer testing of SeNPs on DL cells

2.4.1. Nuclear morphology assay

The peritoneal Daltons lymphoma cell was harvested from Daltons lymphoma bearing mice. Peritoneal exudates cells (PECs) were harvested and adhere for 2 h, Non adherent cells was collected and washed twice with chilled PBS. The DL cell count was adjusted and cultured in RPMI1640 medium supplemented with 10% FBS and antibiotics (penicillin 0.1 µg/µL and streptomycin 0.1 µg/µL) in a humidified incubator with an atmosphere of 95% air and 5% CO_2 at 37 °C with and without LPS and SeNPs for 24 h. Cell were harvested and spread over pre coated air dried poly-lysine coated glass slide, keep slide on room temperature for cell air dry and fix with 4% PFA for 2hr at room temperature Slide was washed and incubated with 0.1% triton X-100 for 15 min followed by washing with PBS and stained for 15 min with DAPI (Sigma, USA). The cell was mounted in anti quenching dye Daboco and observed under confocal microscope.

2.4.2. Confocal microscopy for mitochondrial membrane potential (ΔΨm) by Rh-123

The peritoneal Daltons lymphoma cell was harvested from Daltons lymphoma bearing mice. Peritoneal exudates cells (PECs) were harvested and adhere for 2 h, Non adherent cells was collected and washed twice with chilled PBS. The DL cell count was adjusted and cultured in RPMI1640 medium supplemented with 10% FBS and antibiotics (penicillin 0.1 µg/µL and streptomycin 0.1 µg/µL) in a humidified incubator with an atmosphere of 95% air and 5% CO_2 at 37 °C with and without PMA and SeNPs for 24 h. The cell was harvested and spread over pre coated air dried poly-lysine coated glass slide, keep slide on room temperature for cell air dry and fix with 4% PFA for 2hr at room temperature (RT). Slide was washed and incubated with 0.1% triton X-100 for 15 min, followed by washing with PBS and stained for 45 min with RH-123 dye in dark conditioned at RT, washed with PBS and further stained with Hoechst 33342 for 5 min. Cell mounted in anti-quenching dye Daboco and observed under a confocal microscope.

2.4.3. Flowcytometry for mitochondrial membrane potential (ΔΨm) by Rh-123

The peritoneal Daltons lymphoma cells were harvested form Daltons lymphoma bearing mice. Peritoneal exudate cells (PECs) were harvested and adhere for 2 h, Non adherent cells was collected and washed twice with chilled PBS. DL cell count were adjusted and cultured in RPMI1640 medium supplemented with 10% FBS and antibiotics (penicillin 0.1 µg/µL and streptomycin 0.1 µg/µL) in a humidified incubator with an atmosphere of 95% air and 5% CO_2 at 37 °C with and without LPS and SeNPs for 24 h. Cell was harvested stained for 45 min with RH-123 dye in dark conditioned at RT. The cell was washed twice with 0.1% sodium azide containing 0.1% BSA in PBS for 10 min at 2500 rpm at 4 °C. Further cells were kept in 0.2 ml sheath fluid in ice for Flowcytometry observation (B D Biosciences, Mountain View, CA, USA).

2.4.4. DNA fragmentation assay

The peritoneal Daltons lymphoma cell was harvested from Daltons lymphoma bearing mice. Peritoneal exudate cells (PECs) were harvested and adhere for 2 h, Non adherent cells were collected and washed twice with chilled PBS. The DL cell count was adjusted and cultured in RPMI1640 medium supplemented with 10% FBS and antibiotics (penicillin 0.1 µg/µL and streptomycin 0.1 µg/µL) in a humidified incubator with an atmosphere of 95% air and 5% CO_2 at 37 °C with and without LPS and SeNPs for 24 h. The whole media of cultures were collected and centrifuged at 2500 RPM for 12 min. 50ul TES lysis buffer (20 mM EDTA, 100 mM Tris (pH-8), 0.8%SDS (w/v) in 10 ml distilled water) was added into cultured cell and mix by wide bore pipette, then adds 10ul RNase for 30 min at 37 °C, further 10ul of proteinase K added to the cell and incubate at for 50 °C for 90 min in water bath. 5 ul of 5x loading dye were added to the sample added and observed into 1.5% agarose gel in TAE containing 0.5 µg/ml EtBr.

2.4.5. Flow cytometry analysis of cell cycle progression assay

The peritoneal Daltons lymphoma cell was harvested from daltons lymphoma bearing mice. Peritoneal exudate cells (PECs) were harvested and adhere for 2hr, Non adherent cells was collected and washed twice with chilled PBS. The DL cell count was adjusted and cultured in RPMI1640 medium supplemented with 10% FBS and antibiotics (penicillin 0.1 µg/µL and streptomycin 0.1 µg/µL) in a humidified incubator with an atmosphere of 95% air and 5% CO_2 at 37 °C with and without LPS and SeNPs for 24 h. The cell was harvested and the supernatant was discarded and the pellet was re-suspended in 0.5 ml saponin-propidium iodide (PI) cocktail solution [0.3% saponin (w/v), 25 mg/ml PI (w/v), 0.1 mM EDTA, and10 mg/ml RNase A (w/v) in PBS]. The procedure was carried out in the dark. All tubes were incubated at 4 °C for overnight in dark at 4 °C for 20 min and without washing cells were analyzed by flowcytometry (BD Biosciences, Mountain View, CA, USA) to determine the percentage of cells in each phase of the cell cycle.

2.5. Anti-tumor effect SeNPs on TAMs

2.5.1. Isolation, purification and activation of TAMs

TAMs were harvested from tumor bearing mice as previously described. Briefly, mice were killed by cervical dislocation and TAMs were

harvested by peritoneal lavage as peritoneal exudate cells (PECs) using chilled serum free culture medium RPMI 1640. PECs were harvested by adherent purification in plastic petridishes (Tarson, Kolkata, India) at 37 °C in CO_2 incubator (Shelab, Oregon, CA, USA) for 2 h. The culture was washed thrice with luke warm serum free medium with gentle flushing to ensure that all DL and other non adherent cells were removed and adherent cells were collected. Adherence purified macrophages were seeded in flat-bottom culture flask (Tarson, Kolkata, India) at a cell density of 1×10^6 in the culture medium with or without LPS and SeNPs and incubated for time periods of 24 h in CO_2 incubator.

2.5.2. Cell-adhesion-spreading assay

Cell adherence was evaluated by spreading and attachment assay in order to examine their morphology, adhesion, and fusion. Samples for scanning electron microscopy (SEM) were prepared by standard method as described previously [17]. TAMs were fixed in 2.5% glutraldehyde prepared in 0.1 M sterile PBS (137 mMNaCl, 8.1 mM Na2HPO4·12H2O, 2.68 mMKCl, 1.47 mM KH2PO4) for 30 min and post fixed with 1% OsO4 overnight. After fixation, they were dehydrated using ethanol series. Samples were coated by gold-palladium (Quantum technology- SC7620), and observed using a scanning electron microscope (Zieas-EVO LS-10) at 25 kV at LV mode at central facility of Department of Zoology, BHU, Varanasi, India.

2.5.3. Yeast cell culture

Culture yeast cells in potato dextrose broth for 48 h at 30 °C and autoclave as standard method. Yeast cells wash thrice PBS and centrifuge at 2500 rpm/10 min yeast cells pellet was collected by discarding supernatant and just before use, gently sonicate yeast cells to disrupt clumps and dilute to 10^8 cells/ ml.

2.5.4. Yeast cell bead preparation

Yeast cell was fixed in 4% PFA for 2 h and washed with PBS thrice. The permeability barrier of the plasma membrane was destroyed by treating the cells with buffer (0.01% SDS or 0.3% Triton X-100). Further Yeast cells were incubated in DAPI (10 μg/ml) for fro 24 h at 4 °C, washed with PBS and stored in dark at − 20 °C for further use.

2.5.5. Flowcytometry based phagocytosis assay

Adherence purified macrophages were seeded in flat-bottom culture flask (Tarson, Kolkata, India) at a cell density of 1×10^6 in the culture medium with or without SeNPs and incubated for time periods of 24 h in CO_2 incubator. Further prepared yeast breads were incubated with cells for 24 h. After washing, cells were suspended in 0.1% PBS containing 0.1%NaN3 and then analyzed with a flowcytometry (BD Biosciences, Mountain View, CA, USA) equipped with an Innovate 90-5 (Coherent, Palo Alto, CA, USA) argon ion laser operating at 488 nm and 515 MW in light regulated mode.

2.5.6. DCFDA staining for ROS expression

TAMs were harvested from tumor bearing mice as described above and at a cell density of 1×10^6 in the culture medium with or without LPS and SeNPs and incubated for time periods of 24 h in CO_2 incubator. After that cell was harvested from the medium by centrifugation at 1200 rpm for 10 min, cell washed twice with chilled PBS followed by centrifugation and incubated for 20 min with DCF-DA stain. Cell were spread over pre coated poly-lysine glass slide and air dry and fix, mount with anti-quenching dye DABCO and observed under florescence microscope equipped with FTIC filter.

2.5.7. Fluorescent spectroscopy for estimation of ROS in medium

TAMs were harvested from tumor bearing mice as described above and at a cell density of 1×10^6 in the culture medium with or without LPS and SeNPs and incubated for time periods of 24 h in CO_2 incubator. Cell was harvested from the medium by centrifugation at 2500 rpm for 10 min, cell washed twice with chilled PBS followed by centrifugation and incubated for 20 min with DCFDA stain at the concentration of 20 mM. Cell was harvested from the medium and pellet was discarded and supernatant collected and observed under florescence spectrometer with FTIC filter range using Hitachi f-2500 spectrophotometer at 519 nm in the central facility of Department of Botany, BHU, Varanasi, India.

2.5.8. RNI estimation assay

Nitrite concentration in culture supernatants was determined by a standard microplate assay. Briefly, 50 μl sample (culture supernatant) harvested from cultured medium was seeded into 96-well flat-bottom culture plates and treated with equal volume of Griess reagent (1% sulfanilamide, 0.1% Naphthalene-ethylene-diaminedihidrochloride and 2.5% H_3PO_4) and left for 10 min at room temperature. Absorbance was measured at 540 nm with micro plate reader (Bio-Rad, 680, Bangalore, India). Nitrite concentration was determined by using Sodium nitrite as a standard. The chemicals used for preparation of Griess reagent were obtained from Sigma Chemical Co., St. Louis, USA.

2.5.9. ROI estimation assay

ROI production was determined by measuring H_2O_2 production in the culture supernatant of TAMs cultured in the same conditions of stimulation and pretreatment as in the case of NO·H_2O_2 was measured by the $TISO_4$. Briefly, TAMs were harvested from DL bearing mice as described above and at a cell density of 1×10^6 in the culture medium with or without LPS and SeNPs and incubated for time periods of 24 h in CO_2 incubator. After that cell was harvested from the medium by centrifugation at 1200 rpm for 10 min, cell washed twice with chilled PBS followed by centrifugation. Cells were incubated with $TiSO_4$ (0.1% in 20% H_2SO_4) for 10 min at RT. Supernatant was collected by centrifugation and perform spectrophotometer at 410 nm on ELISA plate reader (Bio-Rad, 680, Bangalore, India).

2.5.10. Flowcytometry analysis

TAMs were harvested from tumor bearing mice as described above and at a cell density of 1×10^6 in the culture medium with or without PMA and SENPs for 24hr of time in RPMI 1640 containing 10% FCS, at 37 °C in 5% CO_2 in humidified CO_2 incubator. Macrophages were suspended in RPMI1640 with 10% FCS, 0.1% NaN_3 and incubated with anti mouseCD14, CD54, CD47,CD172a, RH-123, antibody conjugated with FITC and PE and isotype use as a control conjugated with FITC as per manufacture instruction. After washing, cells were suspended in 0.1% PBS containing 0.1%NaN_3 and then analyzed with a flowcytometry (BD Biosciences, Mountain View, CA, USA)

2.5.11. Statistical analysis

Each value represents the mean SEM of three independent experiments in each group except for in vitro stimulation experiments where two independent experiments were conducted. Data are analyzed by using two-tailed student's *t*-test on statistical software package Sigma Plot, version 12.0. A value of $p < 0.05$ was considered significant.

3. Results

3.1. Characterization of SeNPs

The carboxilc group induced synthesized SeNPs were primarily confirmed by pink color when reduction of sodium selenosulphate. The change in absorption spectra was firstly carried out by UV spectroscopy in the range of 200–350 nm "Fig. 1a". XRD were done for determination of phase composition and crystalline structure of SeNPs. It was found similar to international database of JCPDS file number no- 06-362 "Fig. 1b". The uniform surface structure was observed when SeNPs were further analyzed by SEM at 50 μm scale. The topographic structure of SeNPs surface was found spherical and uniform structure everywhere in the figure "Fig. 2a". The size and shape of SeNPswas done

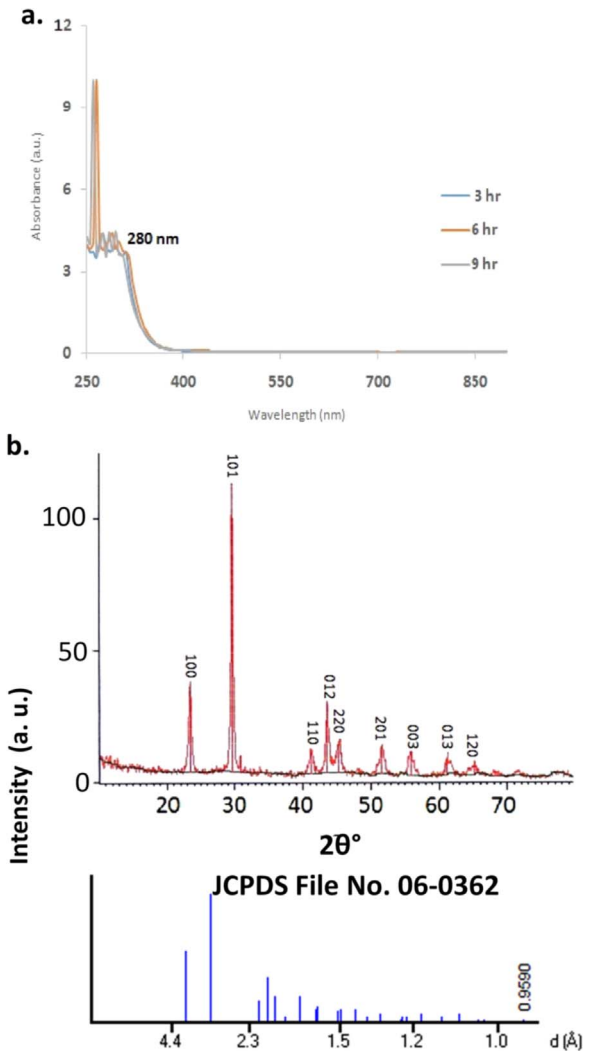

Fig. 1. Figure (a)showing UV–Vis spectra of selenium nanoparticles measured at the time of reaction of sodium citrate with inaqueous solution. The inset is a plot of maximum absorbance versus time of reaction for selenium solution and also the color change of solution before and after addition of sodium citrate (b)XRD pattern of selenium nanoparticles synthesized by sodium citrate. The principal Bragg reflections are identified.

using TEM at 100–200 nm scale "Fig. 2b". It was found that the majority of SeNPs size was found in between 12 and 30 nm in size "Fig. 2c and d". Further FT-IR analysis was carried out to find out the functional group on SeNPs induced by acetic acid shows various absorption peaks at 3434.79. 2380.72, 2345.88, 1996, 1967.1, 1930.38, 1911, 1434.09, 1215.61, 967.66 and 631.03 cm^{-} which represent the functional group such as –NH2, -COOH, CH2, and C=O "Fig. 3a". The thermodynamic behavior of SeNPswas done using DSC thermograph. The carboxlic group induced SeNP shows endothermic and exothermic peaks at different temperature state "Fig. 3b".

3.2. Treatment of SeNPs decreases DL cells proliferation

The anti-tumor effect and dose optimization of SeNPswas done on Daltons lymphoma cells. Prepared SeNPs were lyophilized and dissolved and in PBS and prepare solution in mg/ml, ug/ml and ng/ml of dose for the treatment. Dalton's lymphoma cells (DL Cells) were incubated for with 24 h at the dose concentration of 5–100 mg for the1×10^6cells and cell viability was observed at 6 h, 12 h, and 24 h of incubation using trypen blue exclusion method. It was found that at this concentration the cell viability was found 0.00 at 6 h of treated cells as compare to control group whose cell viability percent value was 93 ± 11 "Fig. 4a". On this dose DL cells were killed and cell proliferation were inhibited but dose was not optimized so further dose of SeNPs was used in ug/ml for 1×10^6 for 24 h. It was found that at this dose concentration at 6 h of incubation the viability of DL cells enhanced but upon increases of time the viability was decrease as compare to control whose viability of 98 ± 10. Finally dose was used in ng/ml for 1×10^6 for 24 h. it was found that more then 40–50% cell viability of was found at the concentration of 5 ng, 10 ng, 20, 30 ng, 40 ng and 50 ng at 24 h of incubation. Further upon screening of the dose, MTT assay was carried out and it was confirmed that a range of ng/ml for 24 h decreases the cell proliferation of DL cell up to 50% "Fig. 4b". On this dose concentration the mitochondrial membrane of DL cells were decreases as compare to control and DNA fragmentation assay shows that this dose inhibits the cell proliferation of DL cells.

3.3. SeNPs affects nuclear morphology

The cytotoxic effects of SeNPs on DL cell lines also examine by observing nuclear morphology. The results showed that the cytotoxicity of SeNPs on DL cells is most potent at 24 h. DL cells were treated with 40 ng dose and compared with the control group of untreated cells, it was found that the nuclear abrogation of DL cell in treating group more as compared to control "Fig. 5a" whose nuclear condensation was found higher and more circular which resulted in significantly higher numbers of cells showing apoptotic feature in tumor cells. SeNPs are capable of inducing apoptosis in DL cells by inducing apoptotic factors.

3.4. SeNPs induces DNA fragmentation and arrest cell cycle progression

DL cells were treated with a previously described dose of AuNPs for the 24 h and nuclear chromatin condensation and DNA fragmentation assay was done. DNA fragments were observed in treating group 1000 bp, 750 bp, 500 bp, 50 bp respectively, as compared to control "Fig. 5b". Further, cell cycle was observed using PI; a DNA binding dye and flow cytometry was done. It was found that the proportions of cells in the G0/G1, S and G2/M phases were 49.0, 23.2, 12.10% in treating cell while in untreated cells the % value of G0/G1, S and G2/M phases was found 40.5, 28.5, 11.1% respectively. This indicated that SeNPs induce the cell arrest in G0/G1 phage which with apoptosis.

3.5. SeNPs decreases mitochondrial membrane potential of DL cells

Mitochondrial membrane potential (ΔΨm) was checked to confirm the apoptosis by using Rhodamine 123, is a cationic fluorescent dye quantity mitochondrial membrane potential (ΔΨm). DL cells were treated with a previously described dose of SeNPs for the 24 h and cell was used to observed ΔΨm by florescence microscopy and flowcytometry. It was found that the intensity of Red dye (Rh-123) decreases as compared to the untreated group of DL cells whose intensity was found high "Figs. 6a and b". Further flow cytometric analysis was performed. Substantial decrease in ΔΨm was observed in treating a group upon exposure to SeNPs which indicates that SeNPs induces DL cell apoptosis via the mitochondrial induction pathway.

3.6. SeNPs enhances the decreased ROS expression of TAMs

Further TAMs were used to check the expression of ROS upon incubation using DCFH-DA staining. It was found that when cell were incubated with SeNPs and compare with control. The co-localization was done and florescence microscopy "Fig. 7a" shows that the ROS generation is found more as compare to untreated and it was further confirmed by FL spectroscopy of cultured supernatant in which the ROS expression was found more compare to untreated control "Fig. 7b".

The Reactive oxygen species contains NO^{-} and H_2O_2 which was estimated by griess method and TISO4 method. Experiments were conducted to examining the effect of SeNPs and incubation time on the

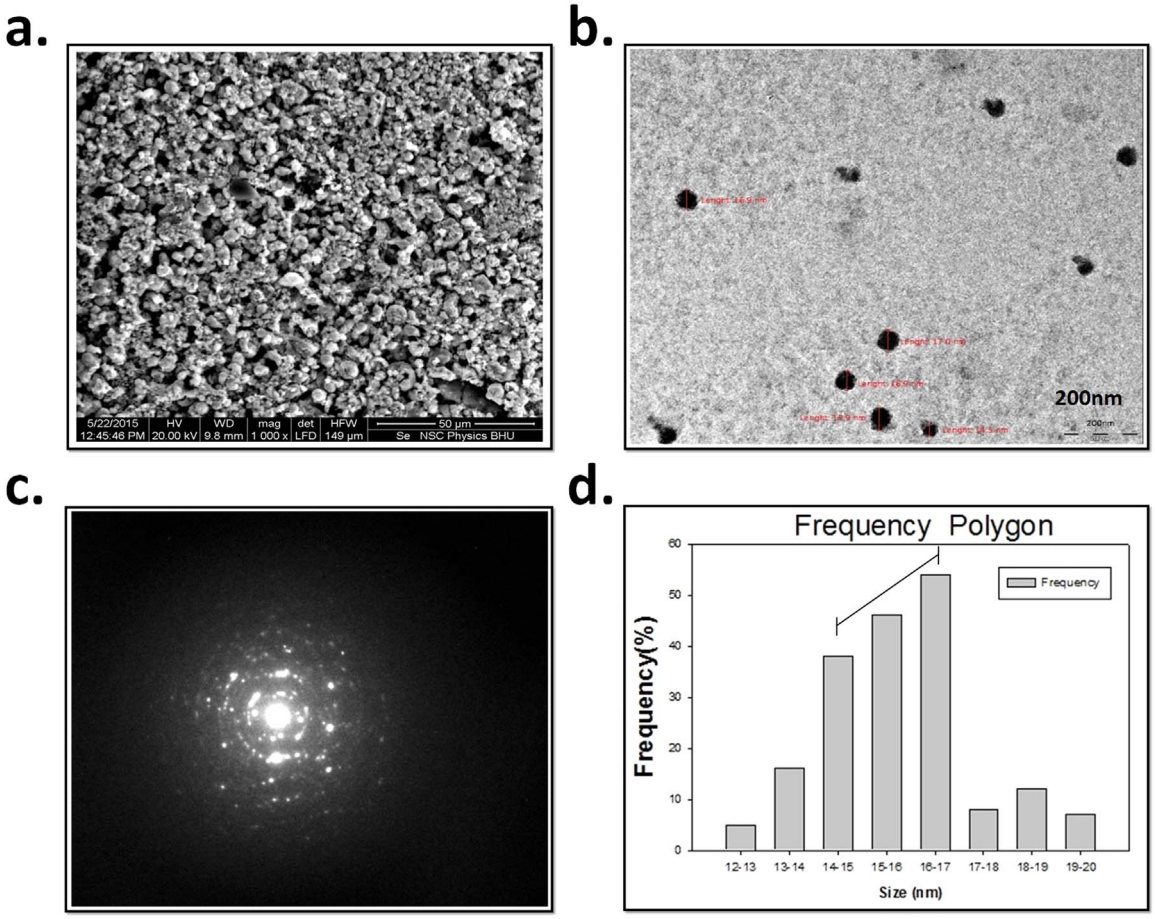

Fig. 2. Figure (a)SEM images of selenium nanoparticles produced by sodium citrate, showing unaggregated and probably aggregated nanoparticles and **(b)** High resolution transmission electron microscopy (HRTEM) images **(c)** of biosynthesized selenium nanoparticles and selected area electron diffraction (SAED) pattern of the nanoparticles showing the rings designated 1, 2, 3 and 4 arisen due to the reflections from (111), (200), (220) and (311) and **(d)**Histogram of percent frequency distribution of selenium nanoparticles.

production of NO_2^-. Results show that TAMs treated with different concentration of SeNPs produces high amount "Fig. 7c" of NO_2^- production as compare to untreated TAMs or compare with untreated SeNPs of macrophage at 24hr of incubation but NO^- production was decrease upon increases of time. It was observed that in other experiments were conducted to examining the effect of SeNPs and incubation time on the production of $H_2O_2^-$. Results shows that TAMs "Fig. 7d" treated with different concentration of Se NPs produces high amount of $H_2O_2^-$ production as compare to untreated TAMs.

3.7. Morphological effects of SeNPs on tumor-associated Macrophages

TAMs were incubated in culture medium supplemented with 10% FBS and activated with SeNPs. To analyze the morphological effect, adherence and lamellipodial extension of SeNPs on TAMs, TAMs were harvested as PECs from DL bearing mice. SEM analysis was done as described in Section 2. Control group of TAMs were spherical in shape and loosely adhered to the surface with less lamellipodia "Fig. 8a". The surface ruffles were almost similar to that of normal resident macrophages incubated in medium only. In contrast, TAMs incubated in culture medium and treated with SeNPs for 24 h showed prominent surface ruffles and narrow cytoplasmic veils. Lamellipodia were more prominent and a large number of cells were spindle shaped, strongly adhered to the surface. Further, polarization of F-actin was significantly enhanced in surrounding punctured of in TAMs, the polarization of F-actin was lesser as compared medium only. On contrary, activation of TAMs with SeNPs showed enhanced polarization of F-actin on the cell periphery of TAMs "Fig. 8b" but lesser compared to unstimulated with SeNPs or LPS. The change in morphology and adherence of TAMs what confirmed by ICAM-1 expression in TAMs and flow-cytometry result shows that the expression of the CD54 (ICAM-1) enhanced in treated group of TAMs as compare to untreated group of TAMs.

3.8. SeNPs enhances the multinucleation and fusion receptor expression

TAMs were harvested as PECs from DL bearing mice by adherence purification as described in material and method. TAMs were incubated in culture medium supplemented with 10% FBS and activated with SeNPs. To analyze the fusion pattern and fusion receptor expression after incubation of SeNPs on TAMs, SEM analysis was done. TAMs were incubated with or without SeNPs and LPS "Fig. 8c". Untreated TAMs shows very less fusion but treated group shows enhanced multinucleation.

Further, effect of SeNPs on the expression of fusion receptor by immunofluorescence TAMs isolated from DL bearing mice were incubated with medium alone or medium containing SeNPs, and expression of fusion receptor CD172α and CD47 was observed by flow-cytometry. Experiments were conducted to examine the effect of SeNPs mediated receptor expression in TAMs harvested from DL bearing mice. It was founded that TAMs treated with SeNPs resulted in significant increase in the expression of "Fig. 9" CD47 and CD172a receptors as compared to the TAMs of CD47and CD172a incubated in medium alone, which is corresponding to ($P < 0.05$) the observation that SeNPs treatment resulted in increase in the tendency of TAMs.

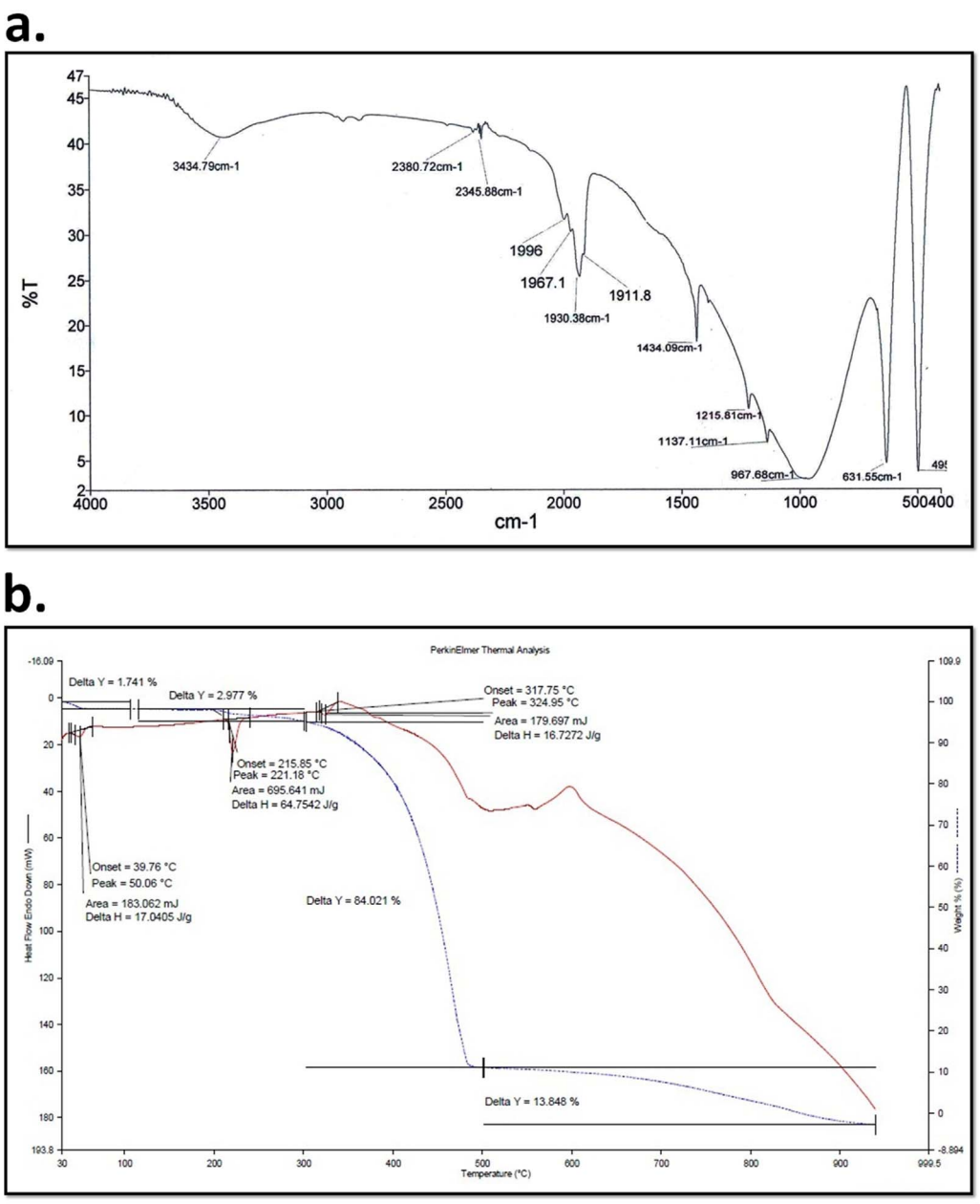

Fig. 3. Typical FTIR absorption spectra of the selenium nanoparticle of the macerated extracellular solution $C_6H_5Na_3O_7{\cdot}2H_2O$.

3.9. SeNPs enhances phagocytosis of TAMs

Effect of SeNPs on the expression of fusion receptor by immunofluorescence TAMs isolated from DL bearing mice were incubated with medium alone or medium containing SeNPs, and phagocytosis index was observed by flowcytometry. Experiments were conducted to examine the effect of SeNPs mediated receptor expression in TAMs harvested from DL bearing mice. It was founded that TAMs treated "Fig. 9" with SeNPs resulted in significant increase in the phagocytosis as compared to the TAMs of incubated in medium alone, which is corresponding to ($P < 0.05$) the observation that SeNPs treatment resulted in increase in the tendency of TAMs.

4. Discussion

In the present study, it is trying to find out the dose optimization of chemically synthesized SeNPs for inhibition of DL cell and optimized anti-tumor dose of TAMs. It was also find out the possible effect on ROS expression in different condition. Our data demonstrate that (i) characterization of chemically synthesized SeNPs and (ii) its dose optimization on DL cell proliferation inhibition done by trypen blue exclusion assay and MTT. There are several method were used to findout the role of NPs on tumor cell, here we are used DNA fragmentation, mitochondrial membrane potential for DL cell apoptosis upon incubation with SeNPs. Antitumor effect of effect and dose optimization was done on TAMs by trypen blue exclusion assay and ROS expression was observed by DCFH-DA staining, Griess method for NO production and TISO4 for H2O2 expression. Adherence, fusion profiling, phagocytosis and receptor expression such as CD47, CD17a and CD54 was done.

Selenium is a trace nutrient play as an essential component of the antioxidant machinery in all cell types for immune system regulation. Selenium is a part of the co-translational incorporation of the amino acid selenocysteine (Sec) into active site of selenoproteins and some of which playing enzymatic functions [26–28]. Selenium has anti-tumor effects in a variety of cancers through mechanisms such as perturbation of tumor cell metabolism, induction of apoptosis, and inhibition of angiogenesis. Moreover, selenium intake has been shown to improve the health status of patients suffering from inflammatory conditions

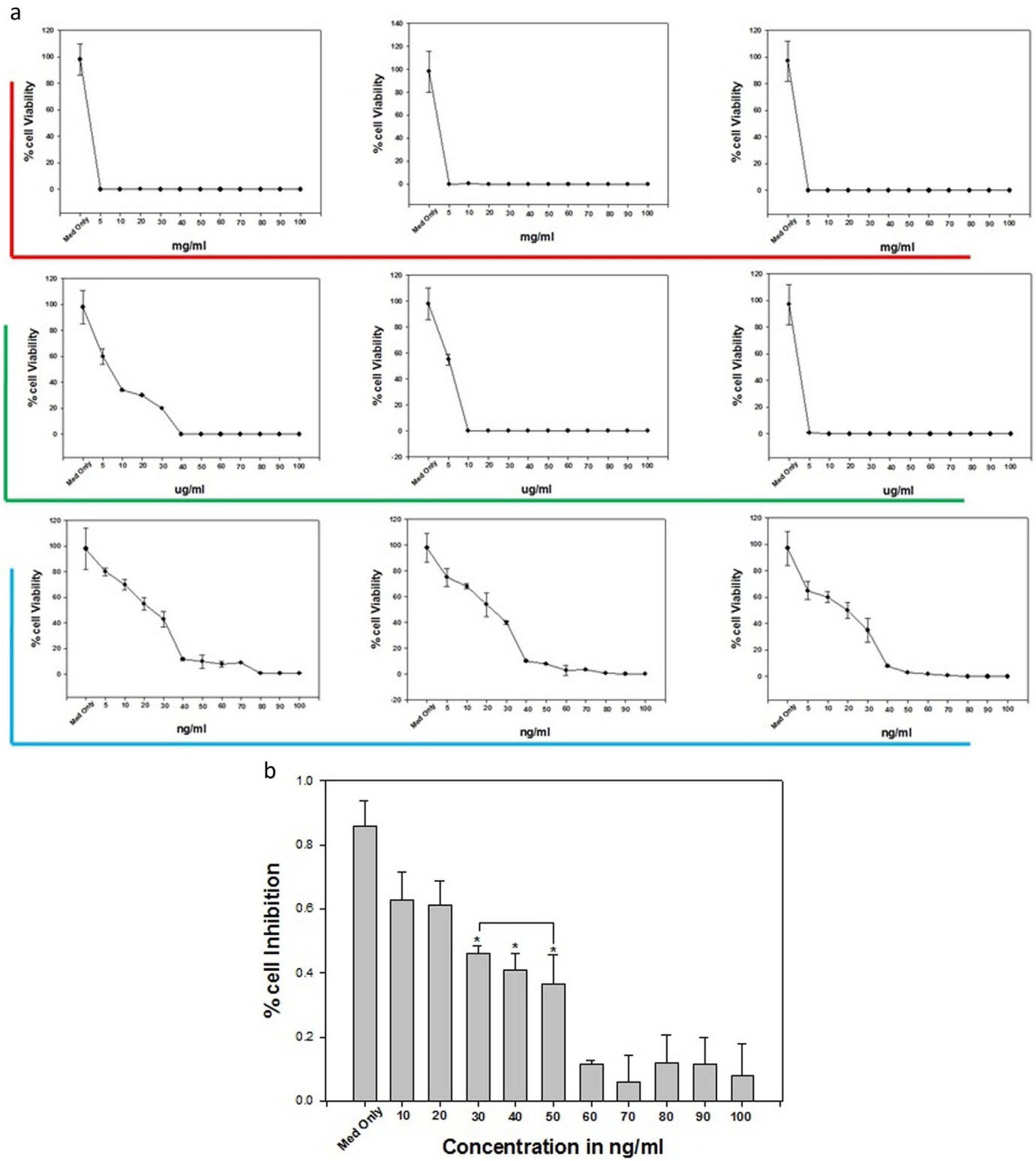

Fig. 4. Figure (a) showing trypen blue exclusion assay for viability of DL cell at different concentration of SeNPs and Figure (b)MTT assay results confirming the in vitro cytotoxicity effect of selenium nanoparticles against the DL cells for 24 h. Data is expressed as mean ± SD of three experiments. Percentage of cytotoxicity is expressed relative to untreated controls (* significant $p < 0.05$).

such as Setoimmune thyroiditis, allergic asthma, and rheumatoid arthritis. These anti-inflammatory actions can be partly explained by the antioxidant role of various selenoproteins, but the precise mechanisms in the context of specific cell types involved in inflammation need to investigation [29]. The carboxilc group induced synthesized SeNPs were synthesized and characterized form our lab (8) and It was found similar to international database of JCPDS file number no. 06-362. The size and shape of SeNPswas done using TEM at 100–200 nm scale. It was found that the majority of SeNPs size was found in between 12 and 30 nm in size. The anti-tumor effect and dose optimization of SeNPs was done on Daltons lymphoma cells. It was found that concentration of ng/ml in which the range of 20 ng to 50 ng for the 10^6 cells more

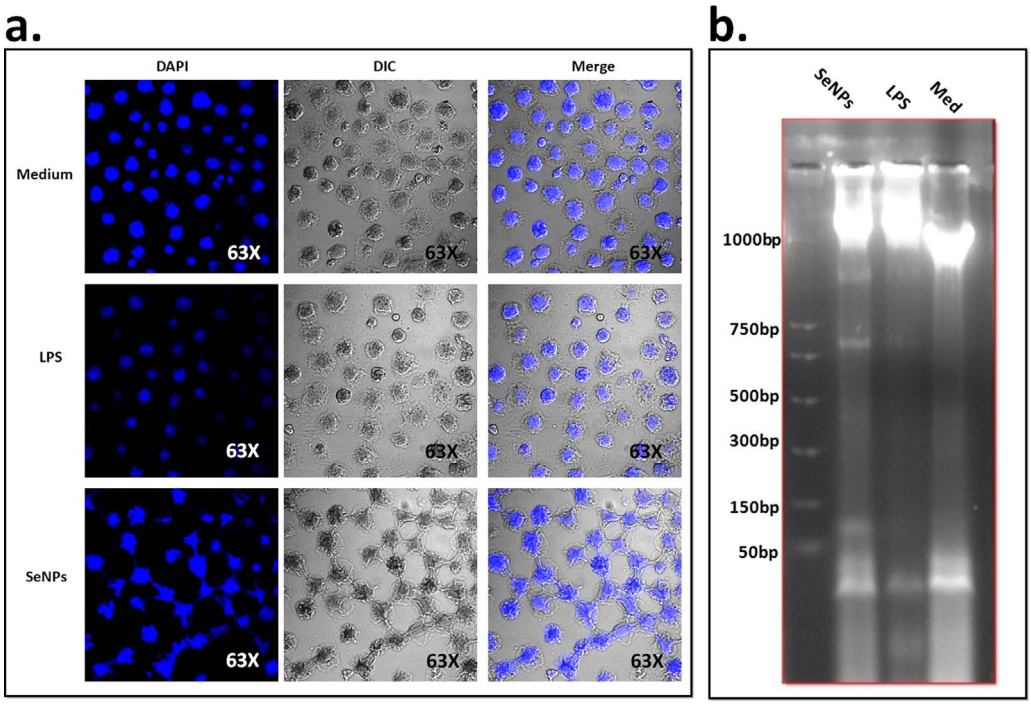

Fig. 5. Figure (a)Confocal microscopic images of selenium nanoparticles induced DL cells nuclear and cytomorphological changes and growth inhibition at different time 24 h. DAPI staining shows apoptotic and necrotic cell death due to the cytotoxicity of biosynthesized selenium nanoparticles while (b) showing estimated concentration of isolated DNA was resolved on 2% agarose along with DNA ladder as shown in the figure and microphotograph were taken under gel-doc system (Bio-Rad) Lane1: DNA ladder; Lane 2: Selenium and Lane 2: LPS; Lane3:Control, respectively.

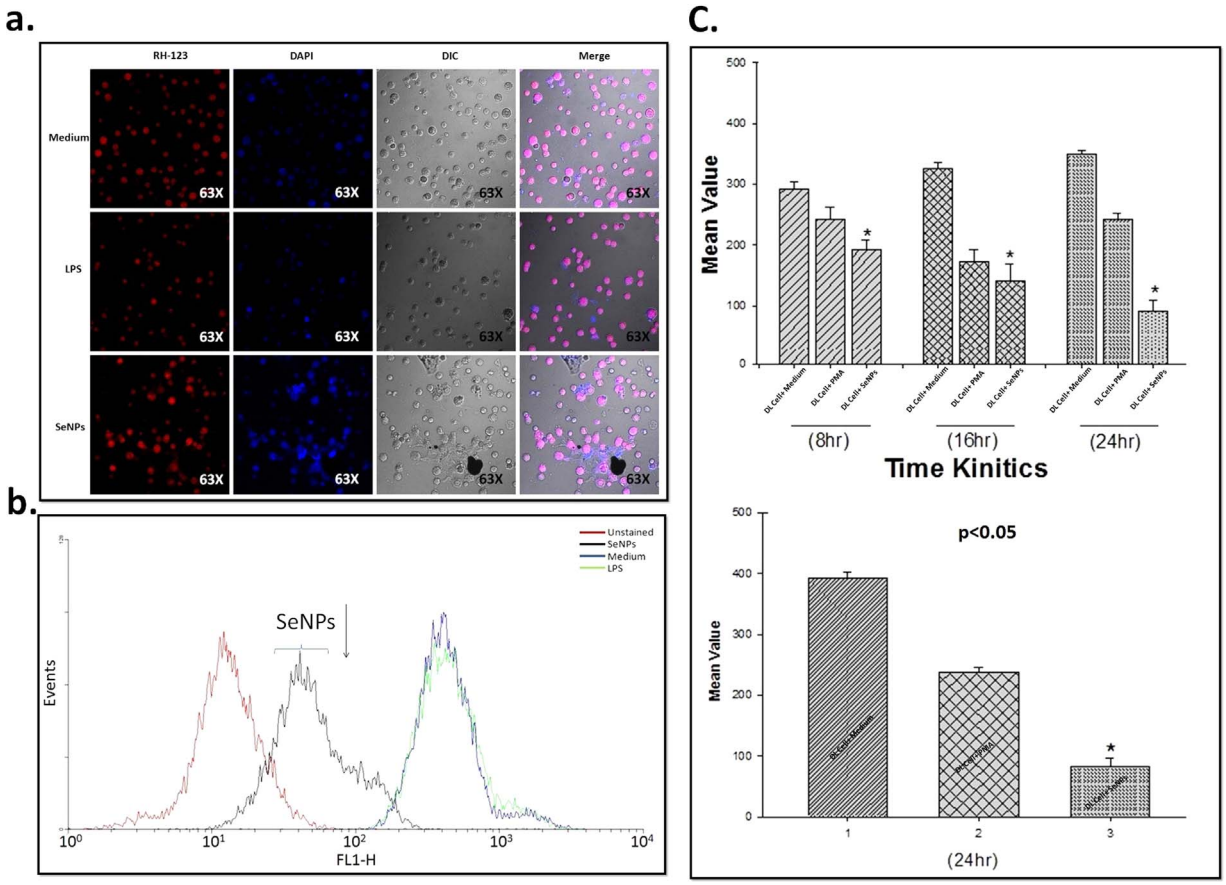

Fig. 6. Fig. (6a) showing Mitochondrial membrane potential analysis (ΔΨm). Confocal microscopic images (a) and flocytometry (b) of selenium nanoparticles induced DL cells and mitochondrial membrane potential (ΔΨm) depolarization was detected at 24 h. Fluorescence was measured via flow cytometry at an excitation wavelength of 485 nm while Fig. (6b) cell cycle asaayoff selenium nanoparticles induced DL cells progression inhibition.

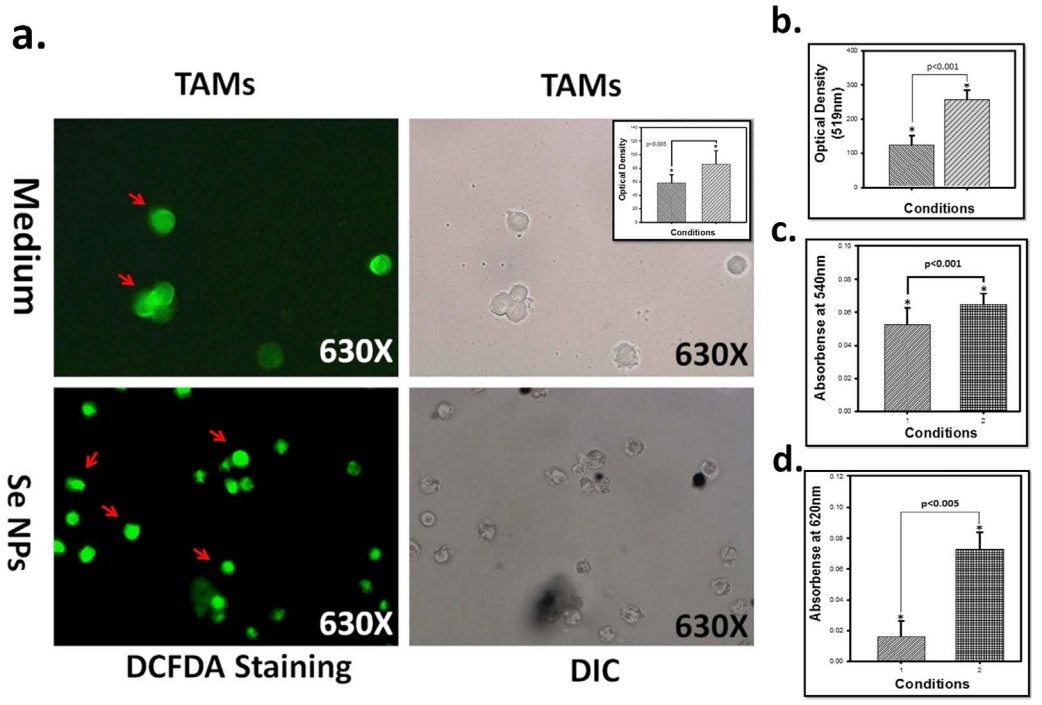

Fig. 7. Figure (a) showing DCFH-DA of TAMs (b) showing ROS expression in supernatant done by FL spectroscopy (C) showing RNI production using griess reagent and (d) showing H2O2 production using TISO4. Data is expressed as mean ± SD of three experiments (* significant $p < 0.05$).

potential value for tumor cell killing. It was confirmed by MTT assay when cell were treated in ng/ml for 24 h. On this dose concentration the mitochondrial membrane of DL cells were decreases as compare to control and DNA fragmentation assay shows that this dose inhibits the cell proliferation of DL cells [30,31].

Further TAMs cell were used to check the dose kinetics on which cells show potent anti-tumor potential. The cell viability and ROS expression was observed. The anti-tumor effect and dose optimization of SeNPs was done on TAMs cell. It was found that concentration of ng/ml in which the range of 20 ng to 50 ng for the 10^6 cell more potential value for tumor cell killing. TAMs were harvested from tumor BALB/C mice as a ascetic fluid in chilled PBS and adhered purified in pre-coated FBS with heat inactivated. Further 1×10^6 cells were taken and 20 ng/ml SeNPs were used for activation of TAMs. Incubated cells with and without SeNPs used for immunocytochemistry of ROS expression and supernatant for FL spectroscopy. It was found that the expression of ROS is enhanced in TAMs with SeNPs treatment more in treated group as compare to without treated group. Similar result were also found when supernatant of treated and untreated group was analyzed under FL spectroscopy it was found that TAMs with SeNPs treatment (263. ± 21.2) more in treated group as compare to without treated group (123. ± 11.2). Further experiment was conducted to examine the production of Reactive Nitrogen Intermediate (NO_2^-) and Reactive Oxygen Intermediate (H_2O_2). Griess method were used for the NO_2^- production and $TISO_4$ were for H_2O_2. It was found that the expression of ROS is enhanced in TAMs (0.087 ± 0.21 NO_2^- for & 0.072 ± 0.11for H_2O_2) with SeNPs treatment more in treated group as compare to without treated group (0.987 ± 0.29 NO_2^- for & 0.072 ± 0.86for H_2O_2). It was reported that, ROS expression was downregulated when the ROS expression was compare with Normal macrophage and TAMs. The suppressed expression was enhanced as upon SeNPs treatment but it was not equal/regain to normal phenotype. ROS are metabolic product of various immune cells such as Mϕ, DC, T cells and almost all tissue. Two cellular organelles are actively participate in the in the production of ROS namely endoplasmic reticulum (ER) and mitochondria. Most of the studies have linked ROS to diseases such as diabetes mellitus, atherosclerosis and cancer. There are several report shows that ROS directly involved to induced DNA damage and it was shown that SeNPs treatment induces the DNA fragmentation of DL cell but enhance the rate of tumor-Sesing mutation and genetic instability [32]. It was also shows that in result that H2O2 excess release results in posttranslation modification of sirf −1 results cell death will take place [33]. The decrease expression of RNS during SeNPs treatment inhibit cell signaling and NF kppa b activation, cell proliferation [34], Further, to see the effect of SeNPs of macrophage phenotype. It was reported that M1 phenotype of macrophages, when adhered to the surface, have prominent lamellipodia, and surface ruffles [35] The macrophages co-resident with tumor cells has not only altered functional states but also morphologically distinct from the normal macrophages. These tumor resident macrophages, also known as tumor-associated macrophages or M2 phenotype, are mostly spherical in shape, loosely adhered to the surface, and have less number of lamellipodia, are absent but they have surface ruffles comparable to that of M1 phenotype of macrophages [36] It is reported that tumor cells produce vast range of immunosuppressive molecules such as IL-4, IL-10, TGF-β, M-CSF, VEGF, MDF, and PGE2 that are able to paralyzing host's immune system leading to inefficient anti-tumor immune response. These immunosuppressive factors polarize the macrophages to TAMs which differs from M1 phenotype in terms of cell surface expression and production of specific and non-specific effector molecules [37]. These immunosuppressive factors not only skewed the purposeful states of the macrophages but also trigger morphological alteration shown by more spherical cell shape, less number of pseudopodia and lacking of cytoplasmic veils greatly suppressing the migration and phagocytic activity and mulitnucleation or giant cell formation of macrophages in the tumor microenvironment [38,39]. Therefore, it is possible to assume that exogenous application of SeNPs to the macrophages may result in the upregulated expression of WASP proteins and activation of CDC42/RAC pathway leading to enhanced actin remodeling and podosomes assembly. However, the effect of SeNPs on the expression of WASP and WIPs/WAVE/SACR family proteins and activation CDC42/RAC pathway is not clear [40]. During infection and malignancies, homotypic fusion to form polykaryon (MGC) or a giant cell which is considered as a hallmark of macrophages. Formation of MGCs is believed to enhance the phagocytic function to limit the spread of infection [41,42]. Giant cells are also important for tissue remodeling, wound healing and removal of even those pathogens which are non-phagocytosable due to increase in size. In the present investigation, we show

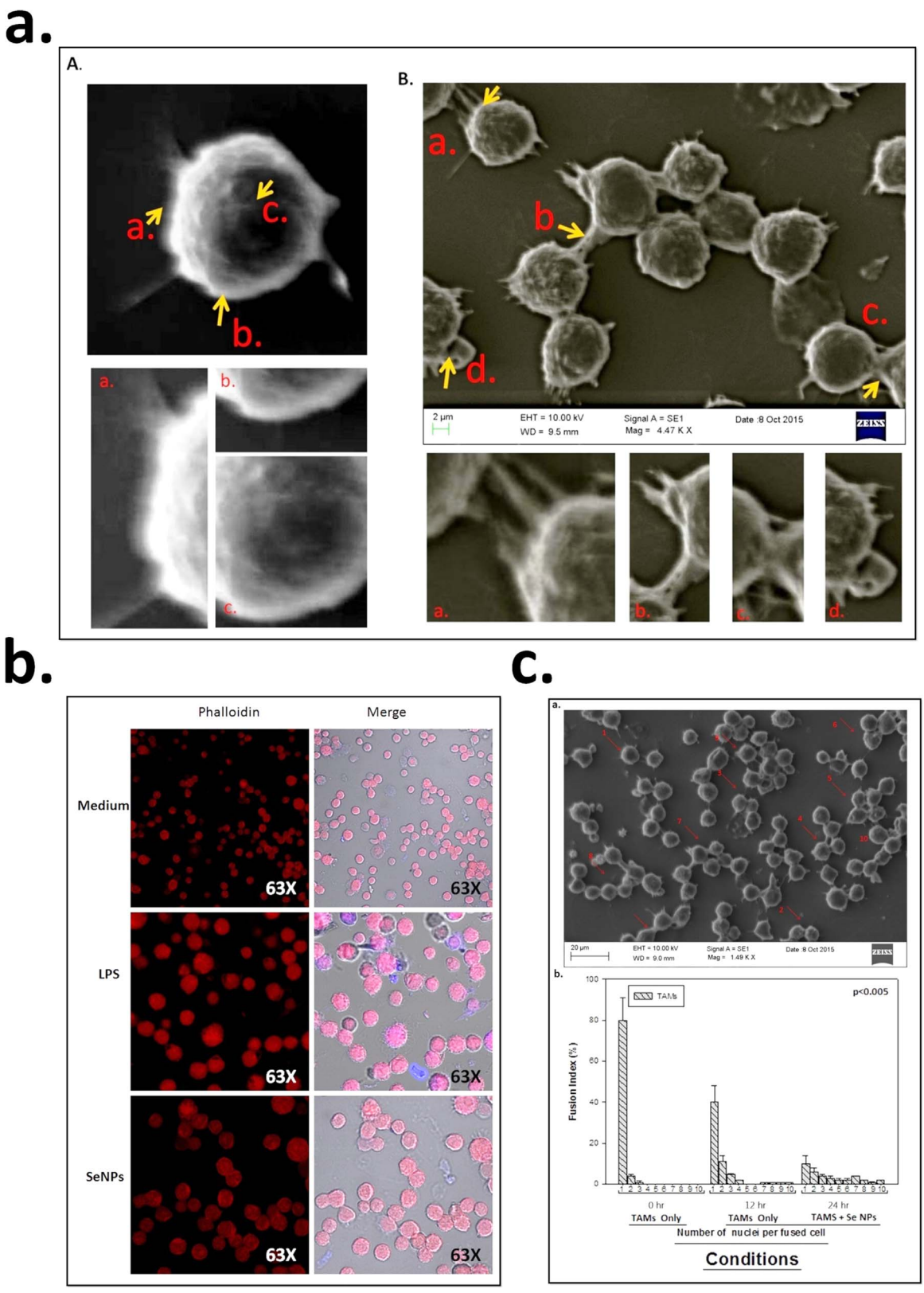

Fig. 8. Figure (a) showing SEM micrograph at 2 µm scale of TAMs with and without treatment (b) showing F-actin expression using confocal microscopy while (C) showing fusion pattern of TAMs. Data is expressed as mean ± SD of three experiments (* significant $p < 0.05$).

that exogenous administration of SeNPs triggers distinct morphological changes and enhances the homotypic fusion of both normal resident and tumor-associated macrophages leading to polykaryon formation. This observation is comparable to well-known role of hsp70 in macrophage activation that leads to the production of proinflammatory cytokines and chemokines in the macrophages [43,44].

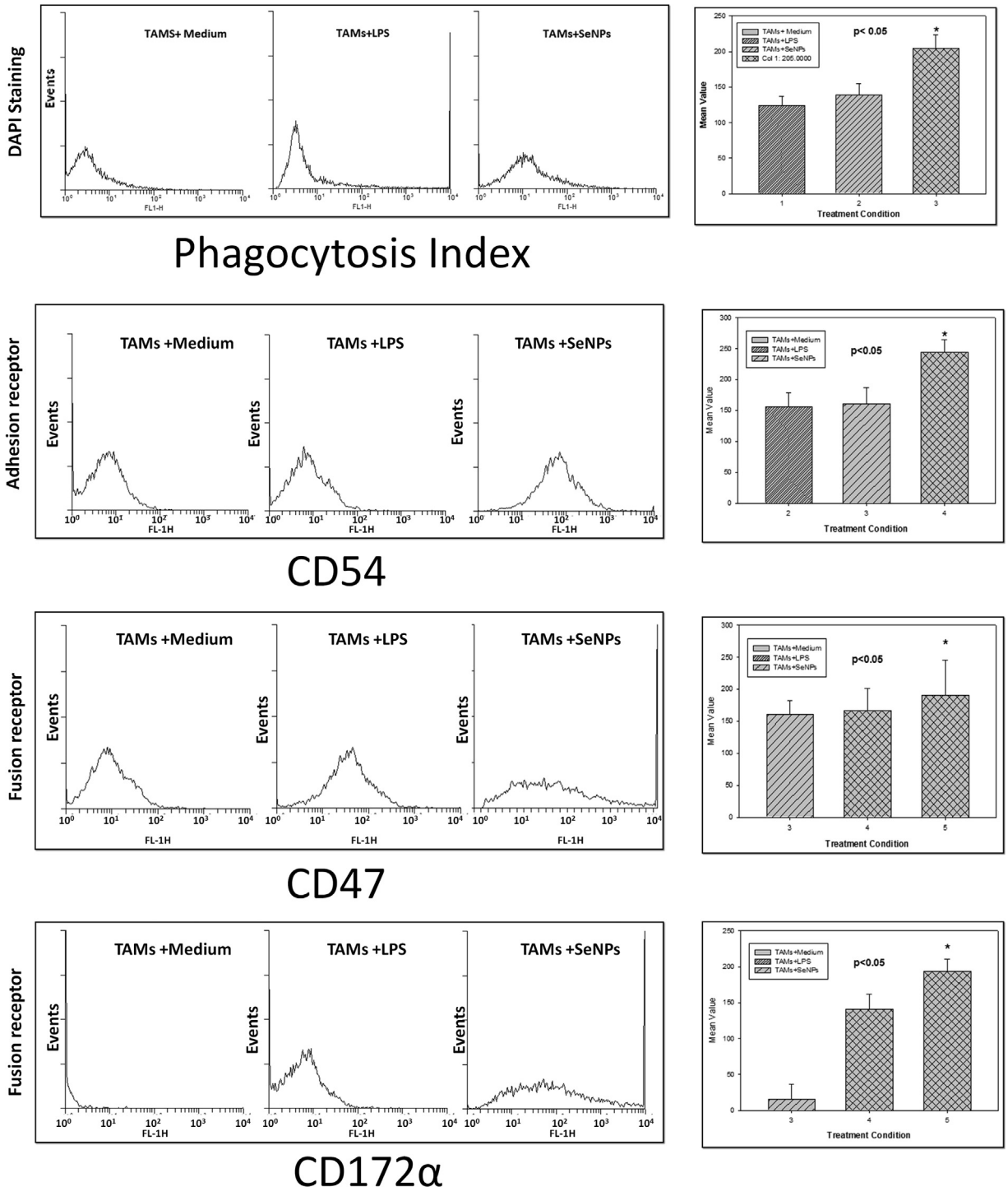

Fig. 9. Figure showing phagocytic index and the expression of adhesion, fusion receptor expression using flowcytometry. Data is expressed as mean ± SD of three experiments (* significant $p < 0.05$).

5. Conclusions and future prospects

Selenium Nanoparticle (SeNPs) is reported that it enhances and maintains optimal immune during infection and malignancies. Keeping the immunomodulatory function of selenium in mind, first characterize and optimize the dose of chemically synthesized selenium nanoparticles (SeNPs) and use to induce TAMs isolated from DL-bearing mice. Results shows that selenium effectively induces the ROS generation, formation of macrophage polykaryon, expression of adhesion molecules (CD54 or ICAM-1), and fusion receptors (CD47 & CD172α) on TAMs. Further, we also found that SeNPs decrease the tumor cell proliferation. SeNPs have potential to induces the anti-tumor function of TAMs whose anti-tumor function down-regulated pliably shifted towards tumor progression. It decreased the proliferation of DL cell by inducing apoptosis. Therefore, the synthesized SeNPs could be used for imaging diagnosis and cancer therapy which must be cost effective with negligible side effects.

Acknowledgements

Authors are thankful to Department of Botany, Banaras Hindu

University for UV-spectroscopy. Department of Chemistry, Banaras Hindu University for FTIR facilities and Professor O. N. Srivastava, Department of Physics, Banaras Hindu University, Varanasi for providing XRD and SEM, TEM facilities. The authors also thankful to Prof. J. K. Roy, Department of Zoology, Banaras Hindu University, Varanasi, for providing the fluorescent microscopy facilities. Dr. Gautam expresses his appreciation to University Grants Commission, New Delhi for student supports.

Funding/support

Supported by UGC, New Delhi, file No. UGC-PDF-2014-15 (9074) for research grant.

Appendix A. Transparency document

Supplementary data associated with this article can be found in the online version at http://dx.doi.org/10.1016/j.bbrep.2017.09.005.

References

[1] P. Jamshidi, S. Soflaei, H. kooshki, Effects of selenium red nanoparticles on LeishmaniaInfantum, cellular apoptosis and inf-γ and IL-4 cytokine responses against visceral leishmaniasis, Adv. Environ. Biol. 8 (21) (2014) 1228–1238.
[2] J.S. Zhang, X.Y. Gao, L.D. Zhang, Y.P. Bao, Biological effect of nano red elemental selenium, Biofactors 15 (1) (2001) 27–38.
[3] M. LaclSestra, A. Navas-Acien, S. Stranges, J.M. Ordovas, E. Guallar, Serum selenium concentrations and hypertension in the US Population, Circ. Cardiovasc. Qual. Outcomes 2 (2009) 369–376, http://dx.doi.org/10.1161/CIRCOUTCOMES.108.831552.
[4] Z. Huang, A.H. Rose, P.R. Hoffmann, The role of selenium in inflammation and immunity: from molecular mechanisms to therapeutic opportunities, Antioxid. Redox Signal 16 (7) (2012) 705–743.
[5] E.T. Mohammed, G.M. Safwat, Assessment of the ameliorative role of seleniumnanoparticles on the oxidative stress of acetaminophen in some tissues of male albino rats, J. Basic Appl. Sci. 2 (2013) 80–85.
[6] M. Aribi, W. Meziane, S. Habi, Y. Boulatika, H. Marchandin, J.L. Aymeric, Macrophage bactericidal activities against staphylococcus sereus are enhanced In vivo by selenium supplementation in a dose- dependent manner, PLOS ONE|PLoS One 10 (9) (2015) e0135515.
[7] V.N. Gladyshev, Selenium: Its Molecular Biology and Role in Human Health (3rd.), Springer, New York, 2006, pp. 99–114.
[8] S. Kumar, M.S. Tomar, A. Acharya, Carboxylic group-induced synthesis and characterization of selenium nanoparticles and its anti-tumor potential on Dalton's lymphoma cells, Colloids Surf. B: Biointerfaces 126 (2015) 546–552.
[9] E.B. Forngaleg-Behia, A.I. Doseff, Regulation of monocytes and macrophages cell fate, Front. Bios 14 (2008) 2413–2431.
[10] C.E. Lewis, J.W. Pollard, Distinct role of macrophages in different tumor microenvironments, Cancer Res. 66 (2) (2006) 605–612.
[11] P.K. Gautam, B.N. Maurya, S. Kumar, P. Deepak, S. Kumar Jr, M.S. Tomar, A. Acharya, Progressive growth of a murine T cell lymphoma alters population kinetics and cell viability of macrophages in a tumor-bearing host, Tumor Biol. 34 (2013) 827–836.
[12] L. Bingle, N.J. Brown, C.E. Lewis, The role of tumor-associated macrophages in tumor progression: implications for new anticancer therapies, J. Pathol. 3 (2002) 254–265.
[13] P.K. Gautam, B.N. Maurya, S. Kumar, Praveen Deepak, S. Kumar Jr, M.S. Tomar, A. Acharya, Progressive growth of a murine T cell lymphoma alterspopulation kinetics and cell viability of macrophages in a tumor-bearing host, Tumor Biol. 34 (2013) 827–836.
[14] N. Volodko, A. Reiner, M. Rudas, R. Jakesz, Tumour-associated macrophages in breast cancer and theirprognostic correlations, Breast 7 (1998) 99–105.
[15] P.K. Gautam, P. Deepak, S. Kumar, A. Acharya, Role of macrophage in tumor microenvironment: prospect in cancer immunotherapy, Eur. J. Inflamm. 10 (1) (2013) 1–14.
[16] P.K. Gautam, B.N. Maurya, S. Kumar, P. Deepak, S. Kumar Jr, M.S. Tomar, A. Acharya, Progressive growth of a murine T cell lymphoma alters population kinetics and cell viability of macrophages in a tumor-bearing host, Tumor Biol. 34 (2013) 827–836, http://dx.doi.org/10.1007/s13277-012-0613-y.
[17] S. Kumar, P. Deepak, S. Kumar, P.K. Gautam, A. Acharya, A benzophenanthridine alkaloid, chelerythrine induces apoptosis in vitro in a Dalton's Lymphoma, J. Cancer Res. Ther. 9 (4) (2013) 693–700.
[18] P.K. Gautam, A. Acharya, Morphological effects of heterologous hsp70 on peritoneal macrophages in a murine T cell lymphoma, Tumor Biol. 34 (2013) 3407–3415.
[19] P.K. Gautam, A. Arbind, Suppressed expression of homotypicmultinucleation, extracellular domains of CD172α (SIRP-α) and CD47 (IAP) receptor in TAMs upregulated by Hsp70-peptide complex in Dalton's lymphoma. scan, J. Immunol. 80 (2014) 22–35.
[20] P.K. Gautam, A. Acharya, Antigenic Hsp70–peptide upregulate altered cell surface MHC class I expression in TAMs and increases anti-tumor function in Dalton's lymphoma bearing mice, Tumor Biol. 36 (2015) 2023–2032.
[21] P.K. Gautam, A. Acharya, Antigenic Hsp70-peptide upregulate altered suppressed expression of docking receptor ICAM-1 in TAMs increases in Dalton's lymphoma bearing mice, IJRST 5 (III) (2015) 86–105.
[22] P.K. Gautam, A. Acharya, Suppressed expression of cd80 (b7.1) and cd86 (b7.2) receptors in tams up-regulated by autologous hsp70– peptide complex in dalton's lymphoma bearing balb/c mice, IJRST 5 (III) (2015) 106–127.
[23] S. Kumar, P.K. Gautam, A. Acharya, Aqueous extract of Withaniasomnifera (ashwagandha) root an indigenous medicinal plant enhances antigen specific cell-mediated immune response (CMIR) in a T cell lymphoma, IJAREAS (2015).
[24] S. Kumar, P.K. Gautam, M.S. Tomar, A. Acharya.CD28 mediated T cell responses is upregulated by exogenous application of autologus hsp70-peptide complex intumor bearing mice.
[25] B. Sarireh, O. Eremin, Tumour-associated macrophages (TAMS): disordered function,immune suppression and progressive tumour growth, J. R. Coll. Surg. Edinb. 45 (1) (2000) 1–16.
[26] F. Ursini, M. Maiorino, C. Gregolin, The selenoenzyme: phospholipid hydroperoxide glutathione proxides, Biochem. Biophys.: Acta 839 (1985) 295–308.
[27] G.V. Kryukov, S. Castellano, S.V. Novoselov, A.V. Lobanov, O. Zehtab, R. Guigo, V.N. Gladyshev, Characterization of mammalian selenoproteomes, Science 300 (2003) 1439–1443.
[28] U.H. Gandhi, N. Kaushal, C. Kodihalli, Hegde S. Ravindra, S.M. Nelson, V. Narayan, H. Vunta, R.F. PSelson, K.S. Prabhu, Selenoprotein-dependent Up-regulation of hematopoietic prostaglandin D2 synthase in macrophages Is mediated through the activation of peroxisome proliferator-activated receptor (PPAR), J. Biol. Chem. VOL 286 (2011) 27471–27482.
[29] F. Gao, Q. Yuan, L. Gao, P. Cai, H. Zhu, R. Liu, Y. Wang, Y. Wei, G. Huang, J. Liang, Cytotoxicity and therapeutic effect of irinotecan combined with selenium nanoparticles, Biomaterials 35 (2014) 8854–8866.
[30] M. Aribi, W. Meziane, S. Habi, Y. Boulatika, H. Marchandin, J.L. Aymeric, Macrophage bactericidal activities against staphylococcus aureus are enhanced in vivo by selenium supplementation in a dose-dependent manner, PLoS One 10 (2015), http://dx.doi.org/10.1371/journal.pone.0135515.
[31] G. Sharma, A.R. Sharma, R. Bhavesh, J. Park, B. Ganbold, J.S. Nam, S.S. Lee SS, Biomolecule-mediated synthesis of selenium nanoparticles using dried Vitisvinifera (raisin) extract, Molecules 19 (3) (2014) 2761–2770.
[32] A.A. Alfadda, M.R. Sallam, Reactive oxygen species in health and disease, J. Biomed. Biotechnol. (2012) 936486, http://dx.doi.org/10.1155/2012/936486.
[33] R. Rajendran, R. Garva, M. Krstic-Demonacos, C. Demonacos, Sirtuins: molecular traffic lights in the crossroad ofoxidative stress, chromatin remodeling, and transcription (ArticleID 368276, 17 pages, 2011), J. Biomed. Biotechnol. (2011), http://dx.doi.org/10.1155/2011/368276.
[34] Assim Disease, A. Alfadda, M. Reem, Reactive oxygen species in health and. Sallam, J. Biomed. Biotechnol. (2012), http://dx.doi.org/10.1155/2012/936486 (Article ID 936486).
[35] P.K. Gautam, A. Acharya, Morphological effects of autologous hsp70 on peritoneal macrophages in a murine T cell lymphoma, Tumor Biol. 34 (2013) 3407–3415.
[36] M.M. Laura, Lamellipodia and fillopodia in metastasis and invasion, FEBS Lett. 582 (2008) 2102, http://dx.doi.org/10.1016/j.febslet.2008.03.039 (PMID: 18396168).
[37] H. Nakagawa, HMiki, M. Ito, K. Ohashi, T. Takenawa, M. Shigeaki, WASP, wave and Mena play different roles in the organization of actin cytoskeleton in lamellipodia, J. Cell Sci. 114 (2001) 1555–1565.
[38] P.K. Gautam, A. Acharya, Suppressed expression of homotypicmultinucleation, extracellular domains of CD172α (SIRP-α) and CD47 (IAP) receptor in TAMs upregulated by Hsp70-peptide complex in Dalton's lymphomaScan, J. Immunol. 80 (2014) 22–35.
[39] M.M. LSera, Lamellipodia and fillopodia in metastasis and invasion, FEBSLett 582 (2008) 2102–2111.
[40] J. Monypennya, HCChoua, I.B. Rodríguezb, J.T. Adrian, I.M. Anton, G.E. Jones, et al., Role of WASP in cell polarity and podosome dynamics of myeloid cells, Eur. J. Cell. Biol. 9 (2011) 198–204.
[41] H. Yamaguchia, F. Pixleyb, C. John, Invadopodia and podosomesin tumor invasion, Eur. J. Cell Biol. 8 (2006) 213–218, http://dx.doi.org/10.1016/j.ejcb.2005.10.004 (PMID:16546563).
[42] J.Y. Shih, A. Yuai, J.-W.C. Jeremy, P.-C. Yang, Tumor-associatedmacrophage: its role in cancer invasion and metastasis, J. Can. Mol. 2 (3) (2006) 101–106.
[43] S. MacLSechlan, E.A. Skokos, N. Meznarich, et al., Macrophage fusion,giant cell formation, and the foreign body response require matrix metalloproteinase 9, J. Leukoc. Biol 85 (2009) 617–626.
[44] P.K. Gautam, A. Acharya, Suppressed expression of homotypicmultinucleation, extracellular domains of CD172α (SIRP-α) and CD47 (IAP) receptor in TAMs upregulated by Hsp70-peptide complex in Dalton's lymphoma, Scan. J. Immunol. 80 (2014) 22–35.